Towards Understanding the Mechanism of PETN Coarsening

Roger Qiu, George Overturf, Richard Gee, Alan Burnham, Brandon Weeks, James De Yoreo

April 7, 2005

Disclaimer

Towards Understanding the Mechanism of PETN Coarsening

S. Roger Qiu[1], George Overturf III[2], Richard Gee[2], Alan K. Burnham[2], Brandon Weeks[3], and James J. De Yoreo[1]
[1]**BioSecurity and Nanoscience Laboratory, Lawrence Livermore National Laboratory**
[2]**Chemistry and Chemical Engineering Division, Lawrence Livermore National Laboratory**
[3]**Department of Chemical Engineering, Texas Tech University**

The long-term goal is to determine the mechanism of PETN crystallization and coarsening at the solid-vapor interface and to quantify the thermodynamic and kinetic parameters that control those processes. We achieve this goal by investigating the surface evolution of synthetic PETN single crystals using *in situ* atomic force microscopy (AFM) at various temperatures.

In this study, we first synthesized high quality PETN single crystals from powder. These crystals were grown from supersaturated organic solution via an evaporation method at a temperature of 5 °C. Representatives of these crystals are shown in Figure 1. All crystals formed from solution had the typical habit of single crystal PETN. These crystals were used as samples for surface evolution studies via AFM.
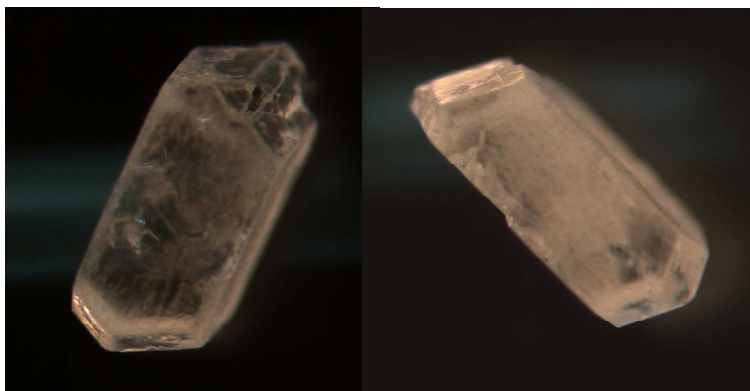

Figure 1. Pictures of bulk PETN single crystals grown from supersaturated solution via solvent evaporation at 5 °C, crystal size ~ 1mm.

The surface morphology of PETN (110) plane at a range of temperatures (22 °C – 50 °C) were investigated using in situ AFM at ambient pressure. The sample was heated in an open environment by a commercially available heating-stage through resistive heating. By monitoring the surface modification at different temperatures, we estimated that PETN started to erode at temperature as low as 24 °C. Because no growth features were observed at temperature above 24 °C, we suggested that the surface erosion were due to sublimation. This result indicated that PETN crystals sublimated even at close to room temperature. It further suggested that if such crystals were stored in a closed system, PETN vapors will be built up and solid-vapor

equilibrium will be reached eventually in the system. Our results also showed the feasibility and capability for the future study in determining the mechanisms that control the sintering process of PETN at the solid-vapor interface in closed environment.

       Images presented below (figs. 2-5) displayed the surface morphological features at different temperatures. AFM images in fig. 2 were collected at 22 °C. At such temperature, there were no observable changes in the surface features with time. In general, at the micron scale, the (110) surface was rather rough, although higher magnification showed flat terraces. Small islands, etch pits, and smooth terraces resided randomly on the surface. Examples were displayed in blue circles/squares. Although terraces with single step were present, the step directions were randomly oriented. Similarly, the shape of the pits and islands displayed in many shapes, but none resembled or related to the shape of the (110) face.
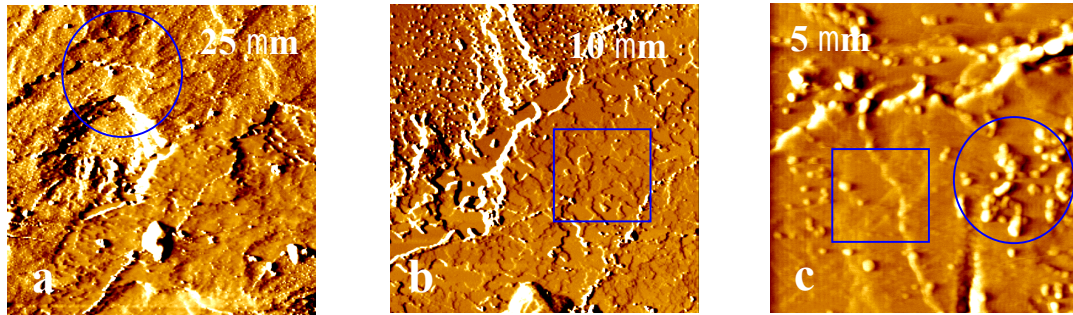

Figure 2. AFM images showing the surface morphology of PETN (110) face at 22 °C at different length scales. The main features are shown in the blue box (circles/squares). (a) Surface features in a 25x25 μm area which includes island, pits, and terraces. (b-c) Surface features shown in at higher magnification, steps, ptis, and islands are clearly discernable. (b) 10 μm and (c) 5 μm.

       Surface features started to change when sample temperature was above 24 °C. The changes were indicated by the recess of step fronts in all directions, the disappearance of existing terraces, and the newly formed pits. Since no growth was observed on the surface at any temperature, it was believed that PETN sublimates at temperature greater than 24 °C. The rate of sublimation increased with temperature. In order to gain quantitative information on sublimation, changes in either terrace areas or formation of pits as a function of time $\frac{dA}{dt}$ for a given temperature were recorded. Temperatures at which these measurements were made are 22 °C, 26 °C, 30 °C, 35 °C, 40 °C, 45 °C, and 50 °C.

       Images in fig.3 showed the example of terrace sublimation as function of time and temperature. For the ease of viewing, the terrace that was followed was emphasized by the blue circles. These images were collected continuously in time while the temperature was increasing. Although this set of data was not suited for rate determination, it clearly showed that PETN sublimated at elevated temperatures by contractions of monolayer islands.

       In order to obtain $\frac{dA}{dt}$ for a given temperature, we collected sequential images at constant (pre-set) temperatures. For example, fig. 4 shows the temporal evolution of surface features at 30 °C. Although the surface is greatly eroded and very rough, we were able to find a feature that could provide dissolution rate information. Such a feature was shown by the blue circles in fig. 4.
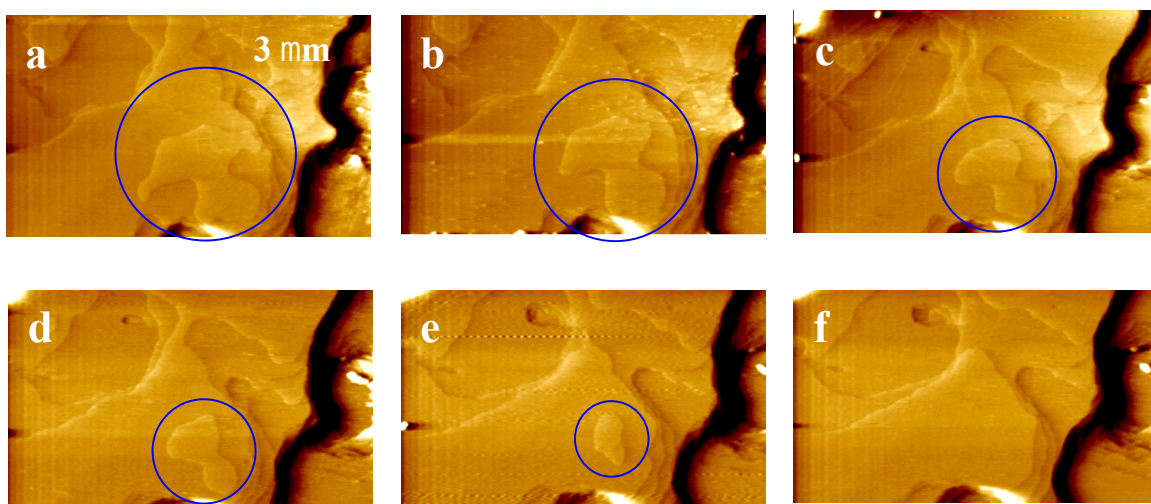
Figure 3. AFM images showing the dissolution of a terrace (inside blue circle) as temperature increases. Horizontal dimension: 3 µm.
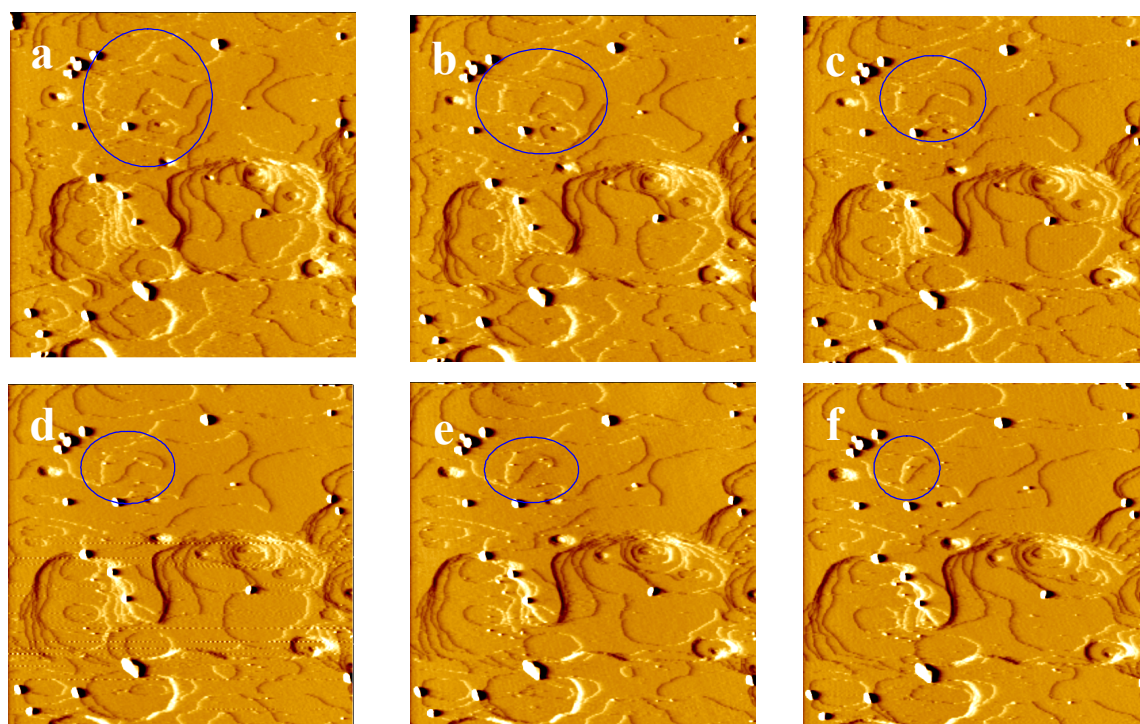

Figure 4. Temporal evolution of surface features at 30 °C. (a) t = 0, (b) t = 10 minutes, (c) t = 21 minutes, (d) t = 31 minutes, (e) t = 42 minutes, (f) t = 52 minutes. The feature inside the blue circles will be used for sublimation rate determination. Horizontal dimension: 4 µm.

At higher temperature (> 40 °C), the surface sublimated so rapidly that pits were formed everywhere. No islands or terraces survived long enough for dissolution rate determination even at the highest available scan rate. Therefore, changes in pits area were used for rate determination. Figure 5 displayed sequential images showing pit evolution at 50 °C. These images would be utilized for rate determination at 50 °C in near future. In addition, more experiments needed to be done at such a temperature so we have better statistics for the rate determination. When sample temperature was higher than 50 °C, the surface dissolved so fast that many small pits were generated at rates such that even at the highest feasible scan rate, one could not catch the change in any given pits. Thus no useful date for rate determination could be collected using AFM. We opted not to conduct any experiment for temperatures higher than 50 °C.

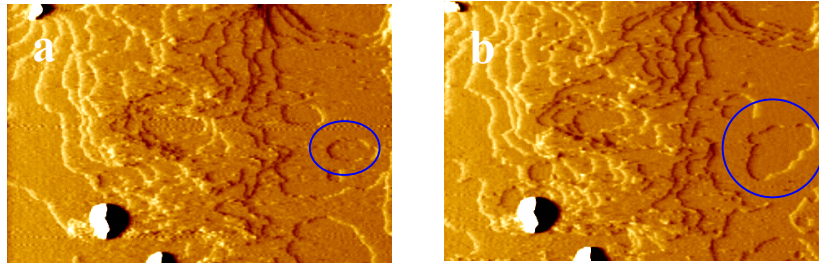Figure 5. Sequential images showing the evolution of pits (inside the blue circles) at 50 °C. (a) t = 0, (b) t = 2 minutes. The changes of the pits area with time will be used for rate determination. Horizontal dimension: 3.5 μm.

We will determine the sublimation rate $\frac{dA}{dt}$ for each temperature we have investigated. For a given temperature, the dependence of $\frac{dA}{dt}$ on time will provide information on the rate limiting factor (diffusion vs detachment) of the decay of the island (1-2). Moreover, we will derive the activation energy barrier from the relationship between $\frac{dA}{dt}$ and temperature.

References

(1) S. Zepeda, S.R. Qiu, G. Gilmer, J.J. De Yoreo, Y. Yeh, and C. A. Orme, "Mechanisms of coarsening and mass transport at the surface of ice", to be submitted.
(2) J. G. McLean et al., Physical Review B, 55 (1997) 1811